Ground Wave Propagation Measurement using DAQ Module and LabVIEW

RISKY MARTIN ANTOSIA

Department of Geophysical Engineering, Sumatera Institute of Technology, Lampung Selatan, Indonesia

Corresponding author: Risky Martin Antosia (e-mail: martin.antosia@tg.itera.ac.id).

ABSTRACT Utilizing a data acquisition (DAQ) module and LABVIEW programming requires to develop in earth science/ engineering and equivalent, especially for educational purposes. This study implemented a geophone and an accelerometer to measure ground wave propagation with a study case of soil surface. Its measurement method consists of two modes. Firstly, the geophone is close to a wave source. Then, its position is changed by the accelerometer. The DAQ converts the detected signals from both sensors and then the LABVIEW interface processes and displays the outputs on the computer. The system can sense and reconstruct waveforms with a steady sampling frequency from 5 to 50 kHz. Also, it can automatically calculate a wave velocity by identifying the rising or falling edges of the wave signal and counting its arrival time within the distance between two sensors. As a result, it produces a better result at an interval of 0.2-0.6 m with a computed wave velocity of 72.531 m/s on average, even though a correction variable should be appended to the outcomes, amplified by two.

KEYWORDS accelerometer; geophone; DAQ module; LabVIEW; wave velocity.

I. INTRODUCTION

THE data acquisition (DAQ) module has been widely used in the industrial and medical fields as well as in education. For example, the DAQ could be applied in the aeronautics [1] and agriculture [2]. In [3, 4], real-time electrocardiogram (ECG) monitoring in the medical field was developed. It could be used as a teaching tool in a laboratory course for educational purposes [5].

On the other hand, a graphical programming language called LabVIEW (Laboratory Virtual Instrument Engineering Workbench) [6–10] was also implemented globally. On the education scale, it could be used for electronics experiment simulation [6–8]. The programming language would provide a decisive outcome when combined with a DAQ module. For example, the engineering students would get real experience in observing the input/ output signal of the sensors and controlling the DAQ through a LabVIEW [11]. Both applications (integration between DAQ and LabVIEW) could be a common need in the industry [12]. In [1], the system for aircraft implementation was developed, in which the graphical user interface organized the data set from the sensors, and [2] built the plant monitoring system that could give an alert or be operated remotely (for agriculture purposes). Then in clinical application, the authors of [3] created an inexpensive device to monitor the ECG signal; and in [4], the system for auto-detection of the signal abnormality related to personal health was enhanced. In [13], the high-speed data acquisition system with a sampling frequency of 200 MB/s for modern tests/measurements in engineering technology was designed.

One of the sensors that can be connected to the integrated DAQ-LabVIEW is vibration/ seismic sensor. The application can be used for analyzing the equipment vibration [9, 14], or the vibration in a drilling activity [10]. An accelerometer is a typical sensor that can be applied as a vibration/ seismic sensor; it can sense ground vibration [15]. Some researchers utilized it for various aims, such as a laboratory scale measurement to calculate the physical

property of the materials [16], sedimentary rocks [17], or igneous/ metamorphic rocks [18], and in situ elastic properties investigation through the wave propagation in the geotechnical field [19, 20]. A geophone can also be occupied as a vibration sensor, yet, the frequency response is less than in an accelerometer [21]. Thus, it is commonly used to detect low-frequency seismic waves. In [22], a system that implemented a triaxial geophone to sense the micro-earthquake wave was built. Then, in [21], the seismic system that applies an accelerometer and a geophone was developed. The output signal of the sensors gave the same response to the ground vibration, although the phase was different. If the accelerometer output is integrated to first-order and the geophone output is derived to first-order, too, each other generates a similar waveform [21].

In general, both sensors can be employed to study the ground's physical properties through wave propagation; wave velocity is one of them. In this study, the author proposes to develop an integrated system to auto-calculation of the rate of the ground wave propagation. Therefore, the system requires sensors, a DAQ module, and LabVIEW as a graphical interface to achieve this objective. Then, the measurement method is adopted from [15, 19]. This system can assist the researchers or students in the activity in earth science, geotechnical, and engineering education fields.

II. MATERIALS AND METHODS

Ground wave propagation can be monitored by setting up vibration/ seismic sensors with a straight line on the ground surface [15]. The assessment can be tested by the hammer hitting the surface with a minimum of two sensors on two points aligned with the impact position [19]. The velocity propagation is calculated as the ratio between the distance of the sensors and the time interval taken by the wave to cover them [19]. Its formula is as follows:

$$v = \frac{d}{\Delta t},\qquad(1)$$

with the unit of velocity propagation (v) in m/s, distance (d) in m, and time interval (Δt) in s. The measurement layout can be viewed in the following figure:
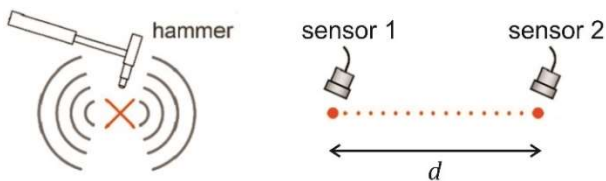

Figure 1. The measurement layout of the ground wave propagation (adapted and modified from [19]).

The system has two main parts: hardware and software designs. The sensors and a DAQ contribute to the hardware. Meanwhile, the software construction will apply LabVIEW, which involves: controlling the DAQ through the computer, data processing, and displaying the outcome on the computer.

The sensors will use a geophone from a work of [21] and an industrial accelerometer from [23]. The difference in implementation of the sensors is in the voltage supply. A geophone does not demand an electrical supply; it is a passive sensor. In contrast, an accelerometer's voltage supply is essential because it is an active sensor. The accelerometer needs a +12 V DC voltage. It is built on a piezo ceramic element, has a sensitivity of 10 V/g, and has a maximum frequency response of about 500 Hz [23]. The piezo element type used for the accelerometer is preferable for field monitoring [15]. After testing the sensor, it has a maximum output of +10 V with an idle output voltage of +5 V.

A DAQ USB-201 will be used for reading the data from the sensors and interfacing it with the LabVIEW; the module is one of the Measurement Computing DAQ family. The module's main features are eight single-ended analog inputs, 100 kS/s maximum sampling frequency, 12-bit ADC resolution, an input voltage range of ±10 V, and it is powered by +5 V USB [24].

The following figure is the schematic diagram of the hardware part. The output line of a geophone is connected to an amplifier (because the output signal amplitude is very low [21]), then attached to analog input channel 0 of the DAQ module. At the same time, an accelerometer is directly connected to channel 1 of the module. The voltage supply of +12 V is put on the accelerometer and has the same grounding line as the DAQ module. It is also a supply to a geophone amplifier to have an equal voltage level with the accelerometer voltage output.
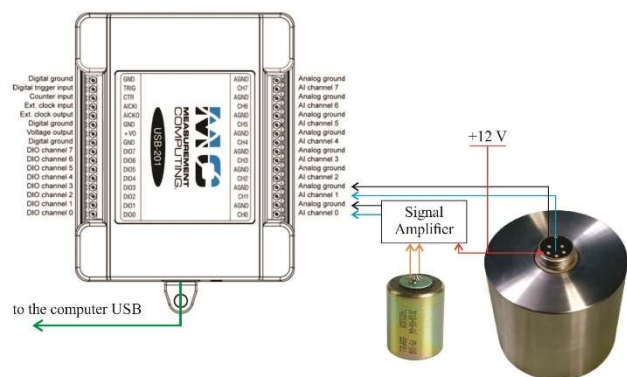

Figure 2. The schematic diagram of the sensors and the DAQ module (modified from [24]).

Figure 3 presents the interface process steps on LabVIEW. The programming is adopted from [25] for accessing the LabVIEW to the DAQ module. On the front

panel of the LabVIEW (Figure 4), there are:
1. The input settings by the user, including:
    a. the sampling rate;
    b. record length (relates to the sample number in the designation time);
    c. trigger level (amplitude level demands to be detected);
    d. distance between the sensors.
2. Output display: time series waveforms, power spectrum, and calculation results (time interval between two sensors and wave velocity).

Since two channels of the DAQ are occupied, each channel has a maximum frequency sampling of 50 kHz (referring to [24]). The block diagram in Figure 5 shows the detailed programming process. In the initialization process, apart from the user settings, there is the fixed-variable adjustment:

1. The number of analog inputs (selected channel 0 and channel 1).
2. Input voltage range (the author employed the ± 5 V because after coupling the sensor's output by the 1μF polar capacitor, it has the output range of about ± 5 V – to obtain the valuable data, it is possible to set the input range value smaller than ± 5 V).
3. Sample mode ("FiniteSample" was chosen).
4. Trigger mode (concerning amplitude level detections of each sensor with the selected means in the LabVIEW "Basic Level Trigger Detection," including the function of "Time," "Falling Edge" for the accelerometer, and "Rising Edge" for the geophone).
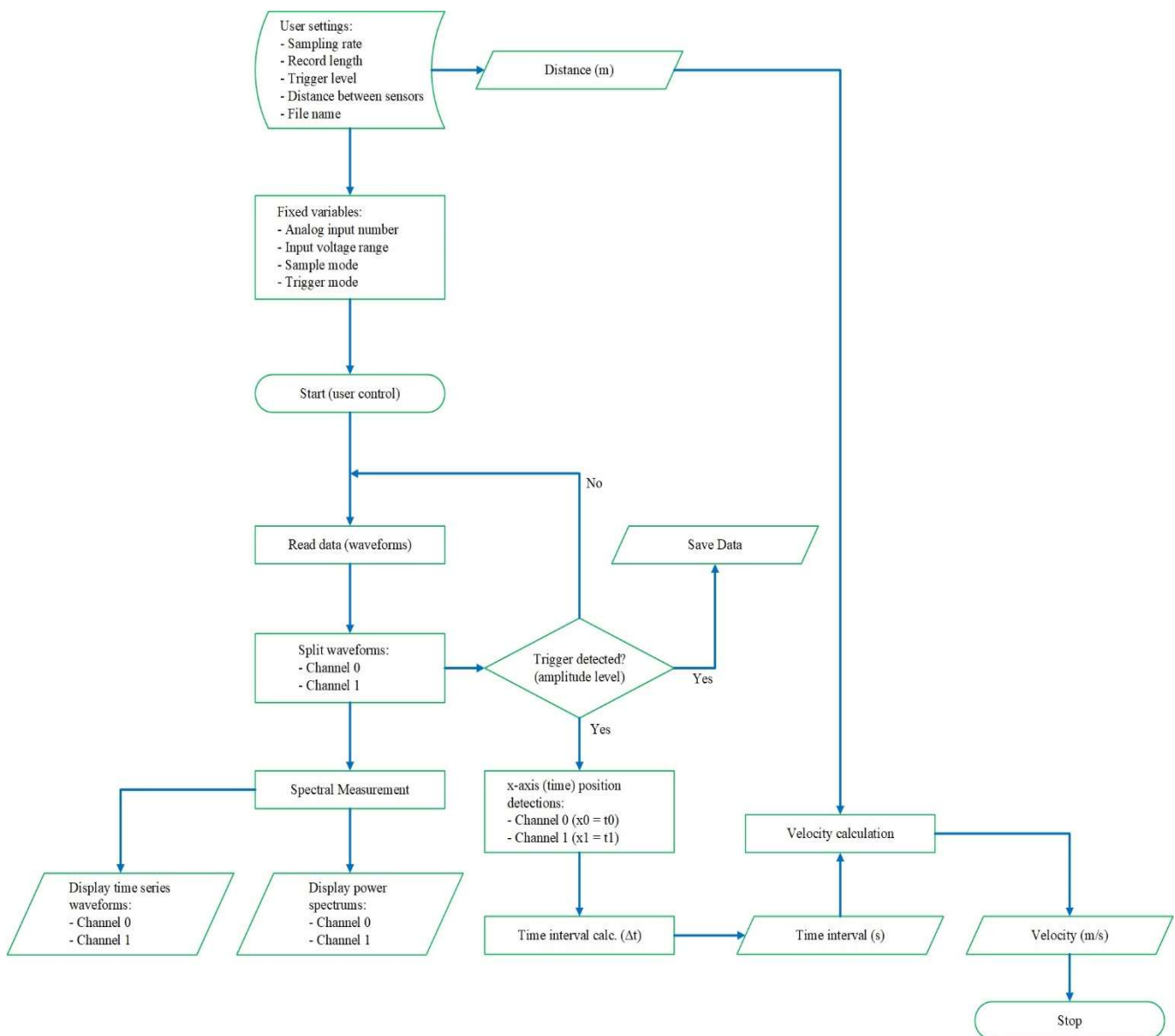
Figure 3. The graphical user interface flowchart on LabVIEW.

The read data process only applies LabVIEW's "Read" function [25]. Its role is to read any incoming input on the DAQ analog inputs with the initialization references arranged before. Since the incoming data are from two analog inputs, the data consists of 2D array waveforms. They are separated in the data processing part to display each waveform and spectral measurement to view the power spectrum graph. The trigger detections (amplitude level) will also work in this part so that the software will run continuously. If the specific voltage values of the sensors are detected (according to the trigger level setting), the time position from each sensor will be identified. Next, the time interval will be measured from the difference of the specified time positions; and the wave velocity can be calculated using Eq. (1). Simultaneously, each sensor's data will be saved to the computer hard drive, consisting of time and amplitude values (for the primary data). After saving the file and calculating the data outcome, the software will stop running (meaning the user needs to click the play button to run the software, and it will be stopped automatically if the condition has been reached).

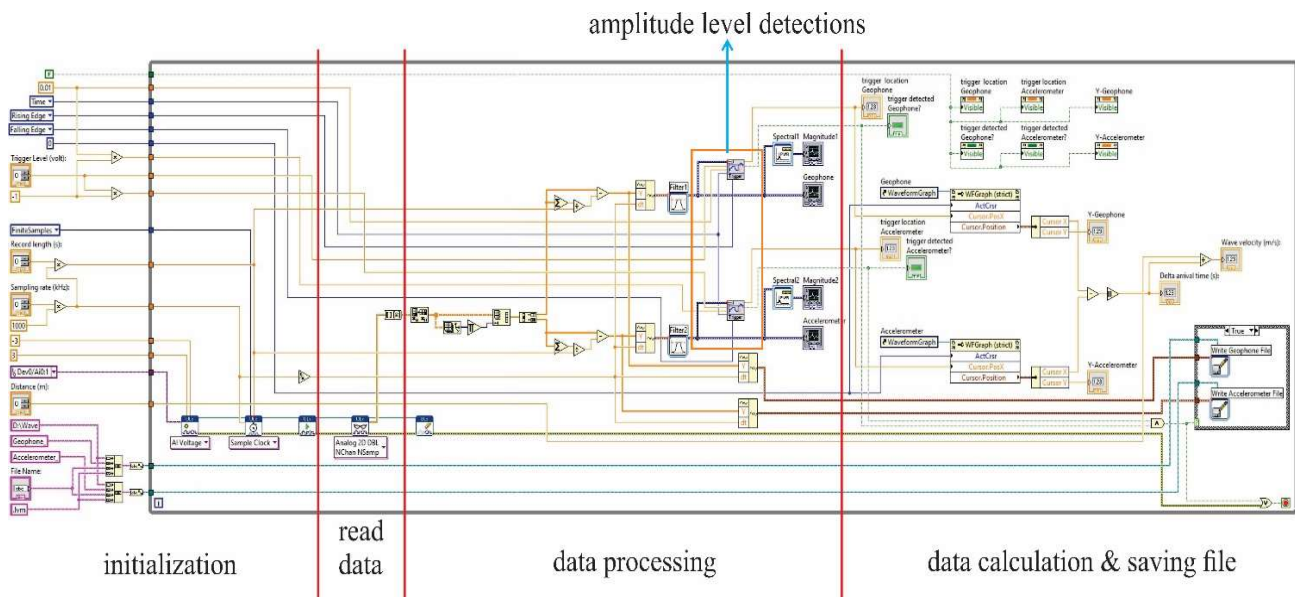Figure 4. The front panel of the software construction on LabVIEW.

Figure 5. The block diagram of the software construction on LabVIEW.

III. RESULTS AND DISCUSSION

The system was tested to observe the wave propagation on the soil surface (Figure 6) with a maximum distance of one meter between two sensors. The system testing procedure implemented fixed and non-fixed spaces with adjustable sampling rates. The measurement length was arranged with the range of 0.2-1.0 m (increment of 0.2 m, refers to [19]), and the sampling frequency was set from one kHz, 5 kHz to 50 kHz (the frequency increment of 5 kHz). Then, the hammer source was alternated near the geophone and accelerometer to ensure the same wave velocity measurements (shift the sensors in Figure 6(b)).

Figure 6(a) displays the software system calibration sample of the time position identification. The condition of the sensors should be at the same point and perpendicular to the vibration/ seismic source. Its outcomes vary from zero to about 0.0007 s between an accelerometer and a geophone. It is reasonable because of the dimension difference between both. The following table presents the average time detection in the calibration mode.

Table 1. The average time determination from different sampling frequencies (F_S) in the calibration test.

F_S (kHz)	average Δt (s)	F_S (kHz)	average Δt (s)
1	0.001	30	0.000567
5	0.0006	35	0.000543
10	0.0006	40	0.000625
15	0.0006	45	0.000667
20	0.0007	50	0.00058
25	0.0006		

Both sensors produce nearly an equal spectrum frequency response (Figure 7), though the accelerometer response delivers a more significant magnitude of over a hundred hertz than the geophone. It means the previous one is better at detecting high-frequency waves. It can be figured from the wave display in time domain mode. For the lower wave frequency, both can be implemented. Overall, both sense the same response at either a low sampling rate or the highest rate without aliasing or over-sampled occurrence.
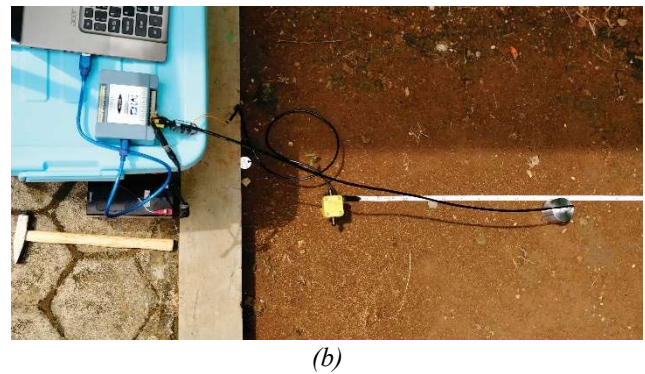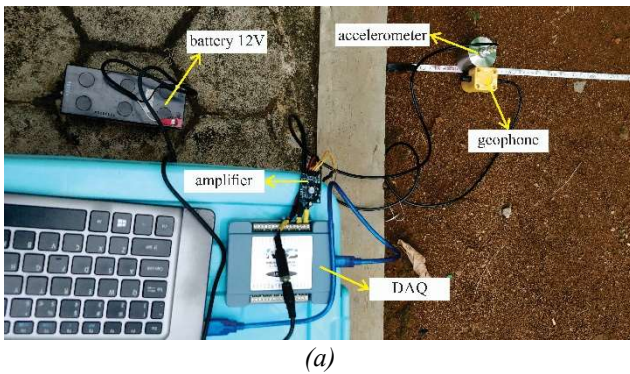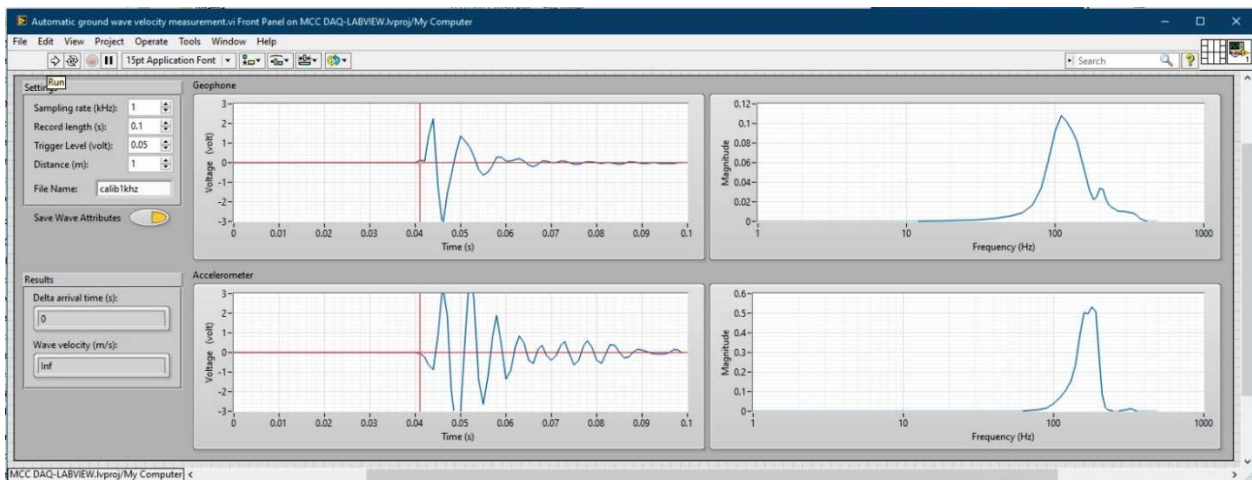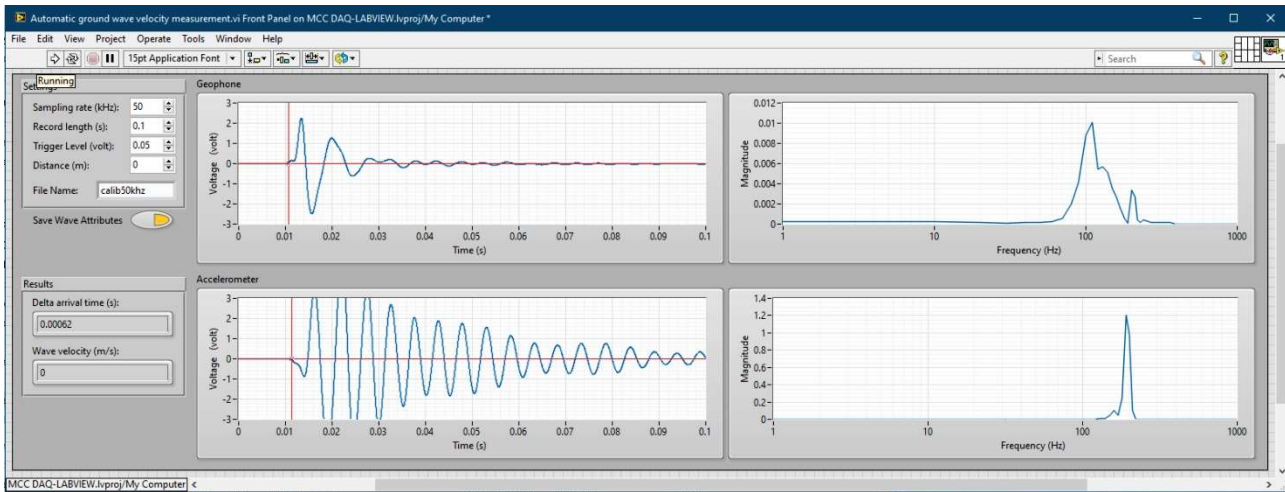

(a)   *(b)*

Figure 6. Field testing: (a) system calibration and (b) ground wave propagation measurement.

(a)

(b)

Figure 7. The resulting example of the system calibration with disparate sampling rates: (a) 1 kHz and (b) 50 kHz.

Moreover, the software successfully obtains the wave arrival time at both sensors in this case. Also, the result indicates a disparate phase between both, corresponding to [21]. To visualize more details, Figure 8 presents the wave response with several selected sampling frequencies at a record length of 10 ms. The image shows that a sampling rate of 5 kHz starts generating a sound construction of a wave, so the higher rate produces better wave reconstruction. This result confirms the statement from the former paragraph. Consequently, the higher the sampling frequency is applied, the more discrete digital data is required to save in a drive/ storage.
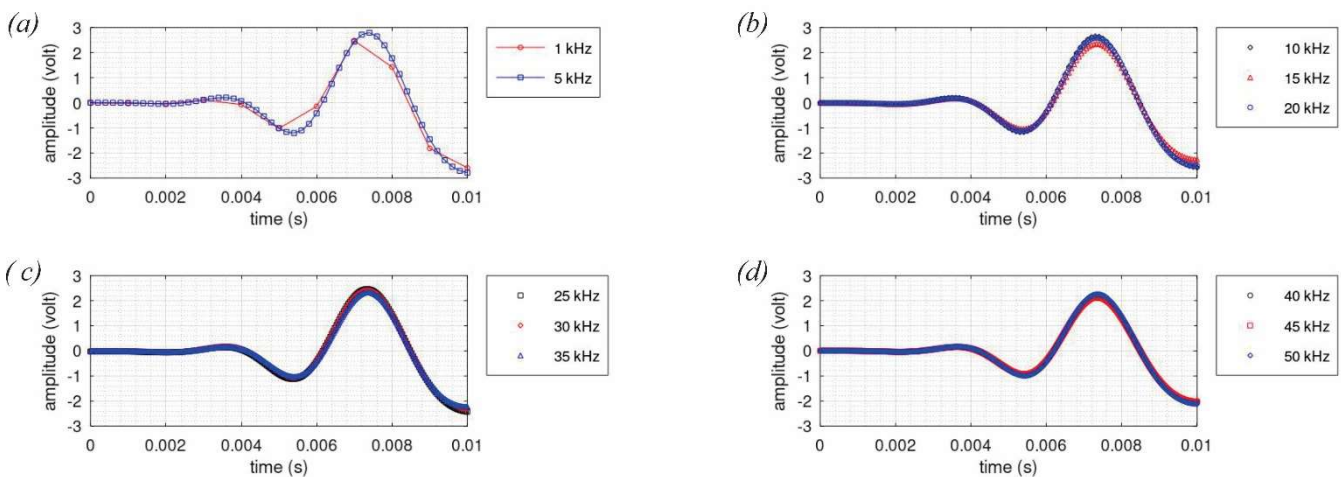

Figure 8. The wave response sample of 10 ms at: (a) 1 kHz and 5 kHz; (b) 10 kHz, 15 kHz, and 20 kHz; (c) 25 kHz, 30 kHz, and 35 kHz; and (d) 40 kHz, 45 kHz, and 50 kHz.

Figure 9 presents the measurement sample of wave propagation using the built software. There are two modes conducted in the measurement field. Firstly, a geophone is the first sensor, and an accelerometer is the second sensor, which means the source is near the geophone. Then, another mode is an alternated position of both sensors. As a result, arrival time detection is a disparity between both modes. Each mode at a distance of 0.2-0.6 m delivers roughly similar (Table 2 and Table 3). The auto-computation wave velocity ranges between both modes at 0.2 m is 62.6-67.1 m/s, at 0.4 m is 74.7-75.4 m/s, and at 0.6 m is 76.0-79.4 m/s; its variance ranges about 1-5 m/s.

Meanwhile, the outcomes give larger discrepancies at 0.8-1.0 m, approximately 30 m/s. This event developed because the geophone was further from the seismic source in the second mode (Table 3). Although an analog signal amplifier was put in the system design, it is not enough to increase the signal power when sensed by the geophone. When a signal is weak, noise can interfere with its ground motion.

If both results of the software-based are averaged for all distances, the velocity has a range of about 63.7-77.7 m/s;

or if the results are generated in the form of linear regression (Figure 10 and Figure 11), each mode produces the following formula:

$$t_{S1} = (1.0798 \times 10^{-2})d + 1.0124 \times 10^{-3}, \qquad (2)$$
$$t_{S2} = (2.0052 \times 10^{-2})d - 1.9309 \times 10^{-3}, \qquad (3)$$

where t_{S1} and t_{S2} are the time functions in each mode (in the unit of s), respectively, and d is the distance between the sensors (m). From those equations, the wave propagation can be derived as follows:

$$v_{S1} = \frac{1}{(1.0798 \times 10^{-2})} = 92.610 \, \text{m/s}, \qquad (4)$$

$$v_{S2} = \frac{1}{(2.0052 \times 10^{-2})} = 49.870 \, \text{m/s}, \qquad (5)$$

where v_{S1} and v_{S2} are wave velocities (m/s) for each mode. The first value is generated higher than the result given in Table 2. Even though such outcomes are presented, it is still reasonable. However, the second value is reasonably far from the displayed data in Table 3 (it can be seen in Figure 11 that the data deviates more from the t_{S2} regression line). It is caused by the previous statement about the sensed capability of the geophone when it is far enough from the wave source.

(a)
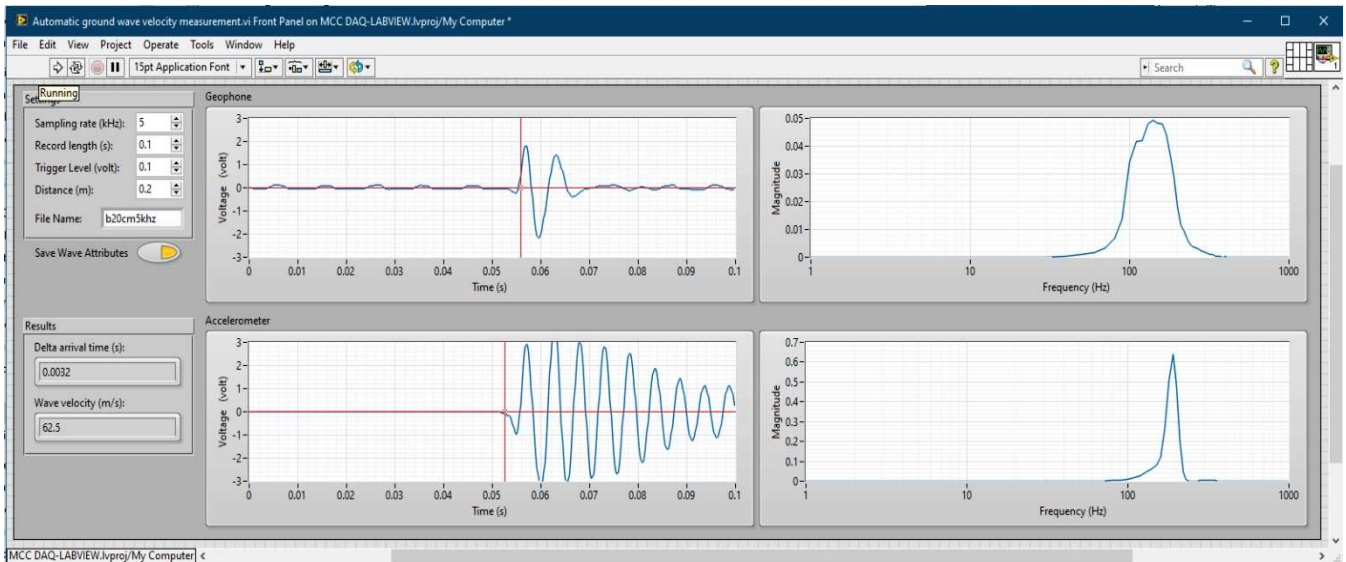
(b)

Figure 9. The resulting example of the system measurement at 5 kHz: (a) a geophone as a sensor one (first mode) and (b) an accelerometer as a sensor one (second mode).

Table 2. The average calculation of all sampling rates at each spacing from the software-based and manual correction in mode 1 (a geophone as the first sensor).

automatic software-based			manual correction	
d (m)	Δt (s)	v (m/s)	Δt (s)	v (m/s)
0.2	0.002981	67.102	0.001246	161.571
0.4	0.005314	75.386	0.002568	156.781
0.6	0.007557	79.447	0.003994	151.454
0.8	0.010332	77.592	0.005297	152.259
1.0	0.011271	88.735	0.00558	179.464
the mean velocity of all intervals (m/s)		77.653		160.306
Std. Dev. (%)		7.786		11.448

Table 3. The average calculation of all sampling rates at each spacing from the software-based and manual correction in mode 2 (an accelerometer as the first sensor).

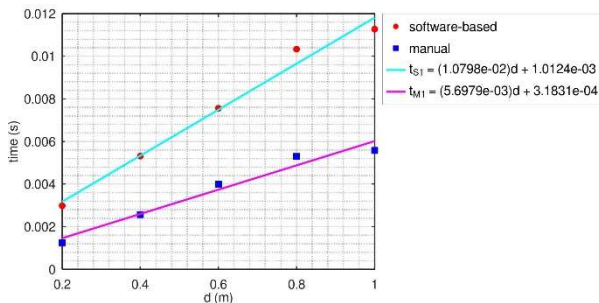| automatic software-based			manual correction	
d (m)	Δt (s)	v (m/s)	Δt (s)	v (m/s)
0.2	0.003199	62.556	0.001373	150.064
0.4	0.005373	74.690	0.002399	168.406
0.6	0.007896	76.006	0.004208	143.301
0.8	0.016186	49.440	0.00552	145.809
1.0	0.017847	56.029	0.005835	171.818
the mean velocity of all intervals (m/s)		63.744		155.880
Std. Dev. (%)		11.572		13.270

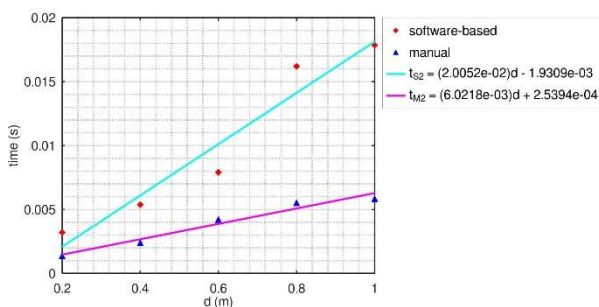Figure 10. Time-distance diagram according to Table 2

Figure 11. Time-distance diagram according to Table 3

According to [26–30], wave velocity at the near surface is approximately under 200 m/s. The automated outcomes from software correspond to the value, but those deviations are appropriately wide. Because of the assumption, the author manually calculated the wave velocity (Table 2 and Table 3), obtaining the velocity range for both modes between 143.3 m/s and 179.5 m/s of all intervals. The values are consistent in their content, with a variance of about 20%. If the velocity is calculated statistically, it delivers at 155.9-160.3 m/s. Even if the value is computed with the same method as in Eqs. (2)-(5) and its viewed graph in Figure 10 and Figure 11 (the parameters are t_{M1} and t_{M2}), its value ranges from 166.1 to 175.5 m/s. Hence, the manual estimation gives almost similar and steady results regardless of the method.

Compared to software-based computation, manual calculations are practically double or trifold. In the first mode, the outcomes should be amplified by a factor of two. There are two categories for the second mode: first, the correction factor is twice at a distance from 0.2 m to 0.6 m; then, for the rest, the outcome values should be triple.

Based on the results from the developed system, the automatic computation of ground wave propagation can be applied to any studies in the field, although the value disparity occurs when compared to the manual method; it needs to employ a correction factor in the results. Apart from the different occurrences, the system can detect the wave arrival time from any vibration sensor. It requires a better means to improve level trigger detection on LABVIEW.

VI. CONCLUSIONS

The system consisting of a DAQ module, and LABVIEW software is developed to measure the ground wave propagation. It has an auto-computation feature to calculate wave velocity and reconstruct waveforms with a steady sampling rate of 5-50 kHz. The essential part of the system is the arrival time detection on the software. Currently, the system can nearly consistently detect the wave arrival time at a distance from 0.2 m to 0.6 m with a computed wave velocity of 72.531 m/s on average. However, a correction factor should be used after acquiring the result from the field.

For further development, the amplifier module should be implemented in the sensor output, whatever its type, especially if employing a geophone; it requires higher signal amplification. Then, the hardware must apply signal filtering in addition to the software. Lastly, the level of the trigger detection on the software should be improved.

References

[1] F. Mujaahid, F. H. A. Anjasmara, R. O. Wiyagi, and K. T. Putra, "Development of data acquisition system using labview-based interface for aircraft application," *Journal of Electrical Technology UMY*, vol. 2, no. 3, pp. 111–115, 2018, https://doi.org/10.18196/jet.2340.

[2] W. Alhalabi, A. Farooq, A. Alhudali, and L. Khafaji, "Case study: 16-channel DAQ device and its application to plant monitoring systems," *Proceedings of the IASTED International Conference on Intelligent Systems and Control*, 2018, vol. 858, pp. 66–74. https://doi.org/10.2316/P.2018.858-006.

[3] M. Murugappan, R. Thirumani, M. I. Omar, and S. Murugappan, "Development of cost effective ECG data acquisition system for clinical applications using LabVIEW," *Proceedings of the 2014 IEEE 10th International Colloquium on Signal Processing and Its Applications, CSPA'2014*, 2014, pp. 100–105. https://doi.org/10.1109/CSPA.2014.6805729.

[4] A. K. Sharma and K. K. Kim, "Real-time ECG signal acquisition and processing using LabVIEW," *Journal of Sensor Science and Technology*, vol. 29, no. 3, pp. 162–171, 2020.

[5] H. T. Evensen, "A versatile platform for programming and data acquisition: Excel and Visual Basic for Applications," *Proceedings of the ASEE Annual Conference and Exposition*, 2014. https://doi.org/10.18260/1-2--20017.

[6] G. R. Gillich, D. Frunzaverde, N. Gillich, and D. Amariei, "The use of virtual instruments in engineering education," *Procedia – Social and Behavioral Sciences*, vol. 2, no. 2, pp. 3806–3810, 2010. https://doi.org/10.1016/j.sbspro.2010.03.594.

[7] H. L. Si, "Design of virtual circuit experiment based on the LabVIEW," *Proceedings of the 2015 International Power, Electronics and Materials Engineering Conference*, 2015, vol. 17, pp. 1118–1121. https://doi.org/10.2991/ipemec-15.2015.206.

[8] W. Wang and X. Quan, "Design of electronic virtual experiment system based on LabVIEW," *IOP Conference Series: Materials Science and Engineering*, vol. 490, no. 4, pp. 1-6, 2019. https://doi.org/10.1088/1757-899X/490/4/042024.

[9] A. K. Desai and A. G. Bharate, "Lab VIEW programming for vibration analysis," *IOSR Journal of Mechanical and Civil Engineering*, vol. 17, no. 01, 2017, https://doi.org/10.9790/1684-17010010105.

[10] M. Yagimli and A. Kaya, "Measurement and analysis of drilling vibration using tracer DAQ and LABVIEW," *Journal of Military and Information Science*, vol. 4, no. 2, p. 45, 2015, https://doi.org/10.17858/jmisci.43356.

[11] A. See, "Utilizing LabVIEW™ for data acquisition and analysis for a 13 weeks undergraduate course," *Proceedings of the ASEE Annual Conference*, 2004. https://doi.org/10.18260/1-2--13654.

[12] I. Sugiarto, T. Thiang, and T. J. Siswanto, "Design and implementation of data acquisition module as an alternative module DAQ LabVIEW," *Journal of Electrical Engineering*, vol. 8, no. 1, pp. 30–37, 2009, https://doi.org/10.9744/jte.8.1.30-37. (in Indonesian)

[13] H. Lew, D. Lv, Y. Zhang, M. Lee, Z. Qin, and X. Zhao, "The design of high speed acquisition and storage system based on labview," *MATEC Web of Conferences*, 2018, vol. 173. https://doi.org/10.1051/matecconf/201817302004.

[14] W. Sun, Y. Zhang, and S. F. Jiang, "Design of data acquisition system of vibration signal for civil engineering structure," *Applied Mechanics and Materials*, 2014, vol. 584–586. https://doi.org/10.4028/www.scientific.net/AMM.584-586.2023.

[15] A. H. Mohammad, N. A Yusoff, A. Madun, S. A. A. Tajudin, M. N. H. Zahari, T. N. T. Chik, N. A. Rahman, and Y. M. N. Annuar, "Ground vibration attenuation measurement using triaxial and single axis accelerometers," *Journal of Physics: Conference Series*, vol. 995, no. 1, pp. 1-9, 2018. https://doi.org/10.1088/1742-6596/995/1/012113.

[16] C. H. Sohn, Y. C. Choi, J. H. Park, D. B. Yoon, and U. P. Chong, "Measuring Young's modulus of materials by using accelerometer," *Transactions of the Korean Society for Noise and Vibration Engineering*, vol. 16, no. 11, pp. 1158–1164, 2006, https://doi.org/10.5050/KSNVN.2006.16.11.1158.

[17] C. McCann and J. Sothcott, "Laboratory measurements of the seismic properties of sedimentary rocks," *Geol Soc Spec Publ*, vol. 65, no. 1, pp. 285–297, 1992, https://doi.org/10.1144/GSL.SP.1992.065.01.22.

[18] T. Elbra, R. Karlqvist, I. Lassila, E. Hæggström, and L. J. Pesonen, "Laboratory measurements of the seismic velocities and other petrophysical properties of the Outokumpu deep drill core samples, eastern Finland," *Geophys J Int*, vol. 184, no. 1, pp. 405–415, 2011, https://doi.org/10.1111/j.1365-246X.2010.04845.x.

[19] J. Marazzani, N. Cavalagli, and V. Gusella, "Elastic properties estimation of masonry walls through the propagation of elastic waves. An experimental investigation," *Applied Sciences (Switzerland)*, vol. 11, no. 19, p. 9091, 2021, https://doi.org/10.3390/app11199091.

[20] K. Matsuoka, K. Kajihara, and H. Tanaka, "Identification of vibration modes and wave propagation of operational rails by multipoint Hammering and reciprocity theorem," *Materials*, vol. 15, no. 3, p. 811, 2022, https://doi.org/10.3390/ma15030811.

[21] R. M. Antosia, R. Sule, and T. Setiawan, "Development of seismic data acquisition systems in Indonesia," *Proceedings of the 11th SEGJ International Symposium, Yokohama, Japan*, 2013, pp. 15–18. https://doi.org/10.1190/segj112013-005.

[22] O. Kafadar, "A geophone-based and low-cost data acquisition and analysis system designed for microtremor measurements," *Geoscientific Instrumentation, Methods and Data Systems*, vol. 9, no. 2, pp. 365–373, 2020, https://doi.org/10.5194/gi-9-365-2020.

[23] Geocis, "Ultra Low Seismic Accelerometer (ULSA)," 2018. [Online]. Available at: http://geocis.net/page.php?ULSA

[24] MCC, "USB-201 Analog and Digital I/O User's Guide," 2019. [Online]. Available at: https://www.mccdaq.com/pdfs/manuals/USB-201.pdf

[25] MCC, "ULx for NI LabVIEW Software Quick Start," 2016. Accessed: Mar. 20, 2023. [Online]. Available at: https://www.mccdaq.com/GetPDF.aspx?t=/PDFs/manuals/QS%20ULx%20for%20NI%20LabVIEW.pdf

[26] W. A. Prakoso, A. Rahayu, I. A. Sadisun, A. S. Muntohar, M. Muzli, and A. Rudyanto, "Comparing shear-wave velocity determined by MASW with borehole measurement at Merapi sediment in Yogyakarta," *International Journal of Technology*, vol. 8, no. 6, pp. 993–1000, 2017, https://doi.org/10.14716/ijtech.v8i6.744.

[27] L. Z. Mase and S. Keawsawasvong, "Seismic hazard maps of Bengkulu city, Indonesia, considering probabilistic spectral response for medium and stiff soils," *The Open Civil Engineering Journal*, vol. 16, no. 1, pp. 1–15, 2022, https://doi.org/10.2174/18741495-v16-e221021-2022-49.

[28] T. Naing, S. Pramumijoyo, and H. Kawase, "Estimation of S-wave velocity structures in Yogyakarta basin, Indonesia," *Journal of Applied Geology*, vol. 1, no. 2, pp. 60–77, 2015, https://doi.org/10.22146/jag.7228.

[29] N. Le Ngal, S. Pramumijoyo, I. Satyarno, K. S. Brotopuspito, J. Kiyono, and E. Hartantyo, "Multi-channel analysis of surface wave method for geotechnical site characterization in Yogyakarta,

Indonesia," *E3S Web of Conferences*, vol. 76, Article no. 03006, 2019. https://doi.org/10.1051/e3sconf/20197603006.

[30] P. S. Thein, S. Pramumijoyo, K. S. Brotopuspito, J. Kiyono, W. Wilopo, A. Furukawa, A. Setianto, and R. R Putra, "Estimation of S-wave velocity structure for sedimentary layered media using microtremor array measurements in Palu city, Indonesia," *Procedia Environ Sci*, vol. 28, pp. 595–605, 2015, https://doi.org/10.1016/j.proenv.2015.07.070.

RISKY MARTIN ANTOSIA *received a bachelor's degree in Instrumentation Physics and a master's degree in Geophysical Engineering. Both degrees are from Bandung Institute of Technology, Indonesia. Since 2019, he has been a lecturer at the Department of Geophysical Engineering, Sumatera Institute of Technology, Indonesia. His areas of scientific interest include instrumentation, computation, and geophysics.*